Core Electron Binding Energies in Solids from Periodic All-Electron $\triangle$-Self-Consistent-Field Calculations

J. Matthias Kahk,[†,§] Georg S. Michelitsch,[‡] Reinhard J. Maurer,[‡,∥] Karsten Reuter,[‡] and Johannes Lischner[*,¶]

†*Department of Materials, Imperial College London, South Kensington, London SW7 2AZ, United Kingdom*

‡*Chair for Theoretical Chemistry, Technische Universität München, Lichtenbergstr. 4, D-85747 Garching, Germany*

¶*Department of Physics and Department of Materials, and the Thomas Young Centre for Theory and Simulation of Materials, Imperial College London, London SW7 2AZ, United Kingdom*

§*Institute of Physics, University of Tartu, W. Ostwaldi 1, 50411 Tartu, Estonia*

∥*Department of Chemistry, University of Warwick, Gibbet Hill Rd, Coventry, CV4 7AL, United Kingdom*

E-mail: j.lischner@imperial.ac.uk

Abstract

Theoretical calculations of core electron binding energies are required for the interpretation of experimental X-ray photoelectron spectra, but achieving accurate results for solids has proven difficult. In this work, we demonstrate that accurate absolute core electron binding energies in both metallic and insulating solids can be obtained from periodic all-electron Δ-Self-Consistent-Field (ΔSCF) calculations. In particular, we show that core electron binding energies referenced to the valence band maximum can be obtained as total energy differences between two $N-1$ electron systems: one with a core hole, and one with an electron removed from the highest occupied valence state. To achieve convergence with respect to the supercell size, the analogy between localized core holes and charged defects is exploited. Excellent agreement between calculated and experimental core electron binding energies is found for both metals and insulators, with a mean absolute error of 0.24 eV for the systems considered.

Graphical TOC Entry

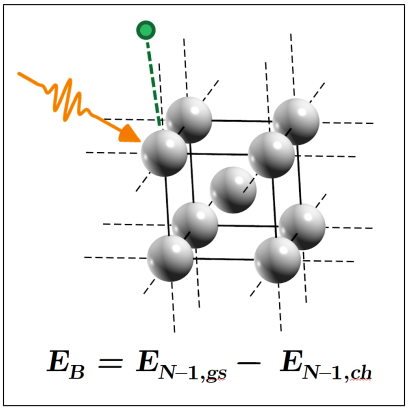

Core level X-ray Photoelectron Spectroscopy (XPS) is a widely used characterization technique that allows insight into the chemical structure of molecules, solids and surfaces. However, theoretical modelling of core electron binding energies is needed to overcome widespread difficulties of interpreting measured XPS spectra in complex materials and this challenge has attracted significant attention in recent years.[1–21] For absolute core electron binding energies of free molecules accurate and computationally efficient methods are now available. For example, the Δ-Self-Consistent-Field (ΔSCF) method based on density functional theory (DFT) has been shown to yield highly accurate results when relativistic effects are properly accounted for and a modern meta-generalized-gradient-approximation (meta-GGA) functional is used.[1–3] It has also been shown that many-body perturbation theory in the form of full-frequency eigenvalue self-consistent GW calculations can yield accurate core electron binding energies in free molecules.[5,6] However, most experimental work is concerned with solids, not gases.

Calculating core electron binding energies in solids has proven to be much more challenging. Even though the ΔSCF method has been known for several decades,[22] periodic all-electron ΔSCF calculations of core electron binding energies have still not been performed. Approximate applications of the DFT-ΔSCF method to periodic systems,[7,8] and G_0W_0 calculations of core electron binding energies in solids[9,10] have been recently reported, but the accuracy of the calculated core electron binding energies in these studies is much lower than the accuracy that has been obtained in studies of free molecules. An alternative approach is to model the solid as a free or embedded cluster.[2,21,23,24] However, in such calculations, the choice of cluster size, shape, and embedding or lack thereof is somewhat ambiguous, and achieving and demonstrating convergence of the calculated absolute core electron binding energies to the limit of infinite cluster size can be difficult. As a result, there is still a need for the development of an accurate and efficient method for the prediction of core electron binding energies in periodic systems.

In this Letter, the application of the all electron ΔSCF method to periodic solids is

demonstrated: the choice of states whose total energies are evaluated in the ΔSCF calculation is discussed, a method for the creation and localization of a core hole in periodic calculations is presented, and the convergence of calculated core electron binding energies to the infinite supercell limit is addressed. Finally, calculated 1s and 2p core electron binding energies in metallic and insulating systems are compared to experimental results.

In ΔSCF calculations of free molecules, the core electron binding energy is calculated as the total energy difference between the N electron ground state, and the $N-1$ electron final state, in which all remaining electrons are allowed to fully relax in the presence of a core hole. The calculated binding energy is referenced to the vacuum level, which is suitable for comparisons against gas phase photoemission measurements. However, in experimental studies of solids, measured core electron binding energies are reported relative to the Fermi level, not the vacuum level.

Two different conventions for referencing calculated core electron binding energies in solids have been proposed in recent theoretical studies. In references[7] and,[8] where the ΔSCF method was used, theoretical binding energies were reported relative to the Fermi level, whereas in recent GW calculations[9,10] theoretical values were reported relative to the energy of the highest occupied valence state. These two conventions are equivalent for metals, but in the latter case, for gapped systems the point of reference is the valence band maximum (VBM). The latter convention is clearly more appropriate. In calculations of insulating solids without defects, the formal Fermi level is typically set to be right in the middle of the band gap. In real materials, however, the position of the Fermi level is determined by defects or impurities in the sample, and it can lie anywhere from the VBM to the conduction band minimum (CBM). Hence, the assumption that the Fermi level lies in the middle of the band gap can lead to very large errors (up to a few eV) in calculated binding energies. If the VBM is used as the point of reference instead, comparisons between theory and experiment are valid regardless of the position of the Fermi level relative to the band edges in the experimental sample.

In principle, the binding energy of a core electron referenced to the energy of the highest occupied state could be obtained from the difference of the results of two ΔSCF calculations: one for the removal of a core electron, and one for the removal of a valence electron. Subtracting these two removal energies yields

$$E_B = (E_{N,gs} - E_{N-1,ch}) - (E_{N,gs} - E_{N-1,gs}) = E_{N-1,gs} - E_{N-1,ch}, \quad (1)$$

where $E_{N,gs}$, $E_{N-1,gs}$, and $E_{N-1,ch}$ denote the total energies of the ground state of the N electron system, the ground state of the $N-1$ electron system, and the core hole state, respectively, and E_B is the calculated core electron binding energy. A key observation is that the energy of the N-electron ground state cancels out in this expression and the core electron binding energy is obtained as the total energy difference between two $N-1$ electron states: the core hole state and the lowest energy state of the $N-1$ electron system. All core electron binding energies reported in this work are calculated using Eq. (1).

All DFT calculations have been performed using the all-electron electronic structure program FHI-aims,[25–27] in which Kohn-Sham eigenstates are expanded in terms of atom-centred basis functions defined on a numerical grid. We have used the SCAN exchange-correlation functional[28] implemented via *dfauto*,[29] and scalar relativistic effects have been accounted for using the scaled Zeroth Order Regular Approximation (scaled ZORA).[30–32] The SCAN functional was chosen as we have previously found it to yield accurate absolute core electron binding energies in free molecules.[2] It is desirable to treat both molecular and extended, as well as metallic and insulating systems at the same level of theory, as many experimental samples contain mixtures of the above, e.g. molecules on metal surfaces. All total energies have been evaluated at the relaxed geometry of the system in the electronic ground state. The serial LAPACK eigensolver as implemented in the ELSI (Electronic Structure Infrastructure) interface was used for solving the generalized eigenvalue problem.[33,34] The direct inversion of the iterative subspace (DIIS) method was used for updating the Kohn-Sham orbitals between successive SCF iterations, with a mixing parameter of 0.2 for insulating

systems and 0.05 for metallic systems.[35,36] Using these settings, calculations with a core hole in a 2p orbital sometimes failed to converge: in those cases, a simple linear mixer with a mixing parameter of 0.15 was used instead. The Kerker preconditioner[37] which is enabled by default in FHI-aims was explicitly turned off in all calculations. Full details of the basis sets and the k-point sampling used in each individual calculation are given in the Supplementary Information.

In order to calculate $E_{N-1,ch}$, it is necessary to allow all remaining core and valence electrons to fully relax in the presence of a spin-polarized, localized core hole. The issue of localizing the core hole requires special attention. The canonical Kohn-Sham orbitals of the core electrons that result from a ground state DFT calculation will be linear combinations of core states localized at all symmetry-equivalent atoms. However, in order to obtain binding energies that agree with experimental measurements, in the calculation of the final state with a core hole, the empty core orbital must be localized at one atomic site by explicitly breaking the symmetry. This issue has been discussed in the context of polyatomic molecules in references.[21,38–41] We have previously proposed a procedure for creating a localized core hole in polyatomic molecules.[2,11] In this study, a slightly modified version of this procedure is used. First, in order to localize one of the core states at a particular atomic site, a fictitious extra nuclear charge of 0.1 e is added to the target atom, and the self-consistent field is allowed to converge in the presence of this fictitious charge. Net neutrality is enforced by adding a compensating uniform background charge. Next, the occupancy of the localized core state is set to zero in one of the spin channels, the fictitious extra nuclear charge is removed, and using the previously obtained Kohn-Sham eigenstates as initial guesses, the self-consistent field is converged again. Again, a compensating uniform background charge is introduced to keep the system neutral. Between SCF iterations, the Maximum Overlap Method (MOM) is used to keep track of the localized core state, in case the energy ordering of the core orbitals changes.[40,42] We emphasize that there are no fictitious charges in the final calculation, and the only constraint that is applied is the non-Aufbau-principle occupation of

the Kohn-Sham eigenstates. We have found this procedure for creating a localized core hole to be highly robust for all materials and core levels that we have considered. The successful localization of a core hole can be verified by visual examination of the wavefunction of the localized core orbital, or alternatively from a Mulliken analysis. As an illustrative example, the localization of the Mg 1s core hole in a $2 \times 2 \times 1$ supercell of magnesium metal is demonstrated in the Supplementary Information.

The spin-unrestricted Kohn-Sham (uKS) formalism is used when calculating $E_{N-1,ch}$. In principle, this can cause issues with spin-contamination - uKS wavefunctions are in general not eigenfunctions of the total spin operator. In this work, calculations of the final states with a core hole were initialized with one more spin-up electron than spin-down electron ($N_{up} - N_{down} = 1.0$), and the total spin was not constrained during the subsequent SCF iterations. We observed that in the converged calculations the total spin moment remained at its initial value, except for some metallic systems where the final value of $N_{up} - N_{down}$ was between 1.0 and 1.1. Mulliken spin analysis indicated that the unpaired electron density was typically almost entirely localized on the atom with a core hole. This is also discussed in the Supplementary Information for the case of a Mg 1s core hole in a $2 \times 2 \times 1$ supercell of magnesium metal. A more advanced treatment of spin would be required for modelling core level spectra of systems with unpaired electrons in the ground state, where complex multiplet structures are often observed. This issue has been recently examined based on the examples of FeO and Fe_2O_3 in [43].

Evaluating the total energy of the ground state of the $N-1$ electron system, $E_{N-1,gs}$, is comparatively straightforward: one electron is removed from the top of the valence band, a uniform compensating background charge is added, and the SCF is converged via standard methods without any constraints. One possible ambiguity arises with regards to the appropriate choice of the spin state for the $N-1$ electron system. When a single electron is removed from a closed-shell system by photoemission, an open-shell system in a doublet spin state is necessarily produced. However, if a fixed spin moment is enforced in a peri-

odic calculation of a solid, the simulated system will have one extra spin-polarized electron per supercell, while the real system only has a single spin-polarized electron in a macroscopic sample region. From a series of numerical tests (see Supplementary Information), we have found that the energy difference between the lowest energy spin-unpolarized state of the $N-1$ electron system and the lowest energy state of the $N-1$ electron system with one spin-polarized hole per supercell vanishes as increasingly large supercells are considered. Therefore, the choice of the spin state of the $N-1$ electron system does not affect the extrapolated core electron binding energies reported on this study, and for the sake of simplicity, spin-unpolarized calculations of the $N-1$ electron system have been performed in all cases. A limitation of the present approach is that it is only applicable to closed shell systems – in calculations of materials with unpaired electrons in the ground state, using the correct spin state when determining $E_{N-1,gs}$ will be important.

Core electron binding energies in periodic solids calculated using Eq. (1) are affected by spurious interactions between periodic copies of the core hole and the uniform background charge. The effect of these interactions can be eliminated by performing calculations of increasingly large supercells, and extrapolating the results to the infinite supercell limit. The nature of the extrapolation depends on whether a core electron is removed from a metal or an insulator. In metals, interactions between periodic images of the core hole are effectively screened by the conduction electrons. Therefore, converged core electron binding energies are obtained when sufficiently large supercells are used. As a representative example of a metallic system, the dependence of the calculated Mg 1s binding energy in Mg metal on the size of the supercell is shown in Figure 1. Figure 1 shows that in bulk Mg, the core electron binding energy is already converged to within 0.1 eV of the infinite supercell limit for a 3×3×2 supercell.

In insulators, the screened Coulomb potential of the core hole is long ranged and decays as $1/r$ in three-dimensional materials, where r is the distance from the core hole. This results in a very slow convergence of the calculated core electron binding energies with respect to

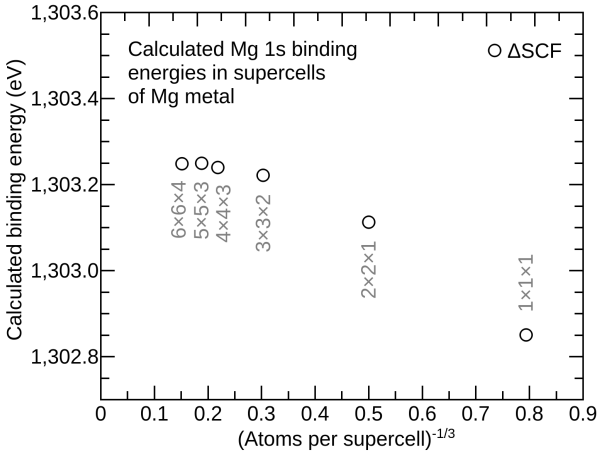

Figure 1: Dependence of the calculated Mg 1s core electron binding energy in Mg metal on the size of the supercell used in the calculation.

the supercell size. However, we have found that graphs of the calculated binding energies versus the inverse cube root of the number of atoms in the supercell (which is proportional to the inverse distance between two periodic copies of the core hole) yield straight lines (when the results for the smallest supercells are excluded). The extrapolated value of the core electron binding energy for an infinitely large supercell is then obtained as the y-axis intercept of these lines. In practice, this is achieved by using a least-squares fitting procedure. As a representative example of an insulating system, the dependence of the calculated C 1s binding energy in β-SiC on the size of the supercell is shown in Figure 2.

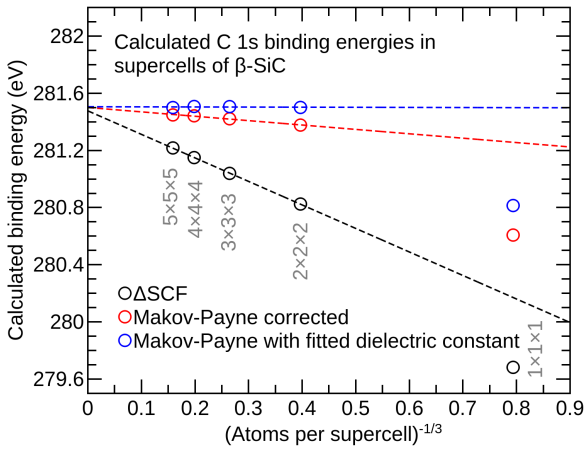

Figure 2: Dependence of the calculated C 1s core electron binding energy in β-SiC on the size of the supercell used in the calculation.

To speed up convergence of core electron binding energies in insulating systems, we make use of finite-size corrections developed in the context of charge defect calculations. In particular, we examine the performance of the correction scheme due to Makov and Payne.[44] In the Makov-Payne scheme, the finite size correction for the total energy is given

$$E_{corr} = \frac{q^2\alpha}{2\epsilon L} - \frac{2\pi qQ}{3\epsilon\Omega}, \tag{2}$$

where q is the defect charge state, α is the Madelung constant, ϵ is the dielectric constant of the material, L is the lattice constant of the lattice formed by the supercells, Q is the quadrupole moment of the charge density induced by the defect, and Ω is the volume of the supercell. The first term is the energy of a periodically repeated point charge in a uniform neutralizing background, scaled by the bulk dielectric constant. The second term depends on the quadrupole moment of the defect charge distribution. In this work, the "defect" is a localized core hole, and its charge distribution can be accurately described by a point charge. In this case, the second term vanishes ($Q = 0$). The value of $q^2\alpha/2L$ can be determined numerically for each supercell (a sample FHI-aims input file is provided in the Supplementary Information). Then, E_{corr} is obtained by dividing this value by the experimental bulk dielectric constant. Published high-frequency dielectric constants (see Supplementary Information) have been used, as the nuclei can be assumed to remain stationary on the time scale of core level photoemission.

The performance of the Makov-Payne correction for C $1s$ binding energies in β-SiC is illustrated in Figure 2. The corrected core electron binding energies are found to show a much weaker dependence on the size of the supercell, and the extrapolated value for an infinite supercell obtained from the corrected binding energies is very similar (difference $<$ 0.05 eV) to the extrapolated value of the uncorrected binding energies.

A modified version of the Makov-Payne correction scheme has been proposed, where an "optimal" value of the bulk dielectric constant, ϵ_{opt}, is chosen such that the size-dependence of the calculated results is minimized.[45,46] For the C 1s core level in β-SiC, we have found

that the plot of the calculated binding energy versus the inverse of the cube root of the number of atoms per supercell becomes flat for $\epsilon_{opt} = 5.33$. The value of the calculated core electron binding energy obtained from the modified Makov-Payne scheme is again very similar to the extrapolated values from the other two methods. More advanced finite size correction schemes[47–51] have been developed for calculations of charged defects, where the defect charge is often spread over a larger area and the Makov-Payne correction becomes inadequate. However, such advanced techniques are not required for the present study because of the strong localization of the core hole.

Similar size-convergence plots for all of the other calculated binding energies reported in this work are provided in the Supplementary Information. For all metallic systems, we have found rapid size convergence of the calculated binding energies. For gapped systems, the three different extrapolation methods described above always give very similar results. A special case is graphite, which is a semimetal. We find that this system exhibits a similar size-convergence as the insulating systems. In the rest of this manuscript, only the extrapolated values of calculated core electron binding energies are discussed.

A comparison between the theoretical core electron binding energies from our ΔSCF calculations and experimentally reported values is presented in Table 1. We emphasize that for all of the gapped systems included in Table 1 both the theoretical and experimental values are referenced to the VBM, not the Fermi level. Experimental binding energies referenced to the VBM were obtained from studies where both the core level and valence band spectra had been recorded. In most cases, excellent agreement between the theoretical and the experimental results is found. The mean absolute error (MAE) for the 15 core electron binding energies considered in this study is 0.24 eV. The MAE for the 11 1s binding energies is 0.29 eV, and for the four 2p binding energies is 0.11 eV. On average, very small errors are obtained for metallic systems (MAE = 0.08 eV), whereas slightly larger errors (MAE = 0.38 eV) are found for insulators. It is worth stressing that a significant part of the MAE for insulators comes from just one material, namely BeO. In BeO, our calculations overestimate

both the Be 1s and O 1s core electron binding energies by approximately 1 eV. Since both core electron binding energies are overestimated by a similar amount, we speculate that the error may be related to the calculation of the ground state of the $N-1$ electron system, which is a shared point of reference. In particular, we hypothesize that DFT with the SCAN functional may fail to accurately predict the position of the VBM in BeO due to the known limitations of semilocal exchange-correlation functionals in describing very ionic materials with large band gaps. Recently, a large quasiparticle correction to the position of the VBM in BeO relative to DFT was reported in.[52] Considerably smaller errors are observed for all other insulators with smaller band gaps, and all metallic systems.

Table 1: A comparison of calculated and experimental core electron binding energies in solids.

Solid	Core level	Theor. E_B (eV)	Expt. E_B (eV)	Ref.	Error (eV)
Li	Li 1s	54.88	54.85	[53–56]	0.03
Be	Be 1s	111.88	111.85	[57]	0.03
Na	Na 1s	1071.56	1071.75	[56,58,59]	−0.19
	Na 2p	30.65	30.51		0.14
Mg	Mg 1s	1303.25	1303.24	[57,60–64]	0.01
	Mg 2p	49.69	49.79		−0.10
Graphite	C 1s	284.44	284.41	[65–69]	0.03
BeO	Be 1s	110.79	110.00		0.79
	O 1s	528.86	527.70	[68,70]	1.16
hex-BN	B 1s	188.42	188.35	[68,71]	0.07
	N 1s	396.39	396.00		0.39
Diamond	C 1s	284.43	284.04	[72–75]	0.39
β-SiC	Si 2p	99.24	99.20	[76–78]	0.04
	C 1s	281.48	281.55		−0.07
Si	Si 2p	99.17	99.03	[79,80]	0.14
				Mean Absolute Error = 0.24 eV	

It is interesting to compare the DFT-ΔSCF method for predicting core electron binding energies in solids to the GW method, that was used in references[9] and.[10] The GW approach has been highly successful at predicting the binding energies of valence electrons, and it is known to solve the famous band gap problem in DFT. The use of the GW method for the calculation of core electron binding energies was investigated in detail in references[5] and,[6]

and it was shown that G_0W_0 calculations with a PBEh45 starting point or eigenvalue-self-consistent GW calculations can yield accurate absolute core electron binding energies in molecular systems. However, these studies also found that a full-frequency treatment of the self-energy is essential to obtain meaningful results, that G_0W_0 calculations of core electron binding energies show a very strong dependence on the mean-field starting point, and that an extrapolation to complete basis set limit is needed to obtain converged results. In comparison to the GW approach, the principal advantage of the DFT-ΔSCF method is its significantly lower computational cost which enables the study of core electron binding energies in complex materials, such as surfaces with adsorbates, clusters or materials containing defects. However, we also note that the mean absolute error found in this work (0.24 eV) is significantly lower than the mean absolute errors reported in previous GW calculations of absolute core electron binding energies in solids (0.53 eV and 0.57 eV eV in references[9] and[10] respectively). The main motivation to go beyond the DFT-ΔSCF approach arises when information about the full spectral function, including satellite peaks is required. Formally, the total energy differences from ΔSCF calculations correspond to quasiparticle energies from many body perturbation theory.

The results presented in this study highlight the versatility of the DFT-ΔSCF approach for predicting accurate absolute core electron binding energies in materials. In particular, they demonstrate that the same computational framework that was previously found to yield accurate absolute core electron binding energies in molecular systems also produces good results for both metallic and insulating solids. As many experimental XPS studies are performed on solids, this work establishes periodic ΔSCF calculations as a powerful technique for guiding the interpretation of experimental core-electron photoemission spectra.

Acknowledgement

J.L. and J.M.K. acknowledge funding from EPSRC under Grant No. EP/R002010/1 and from a Royal Society University Research Fellowship (URF\R\191004). This work used the ARCHER UK National Supercomputing Service via J.L.'s membership of the HEC Materials Chemistry Consortium of UK, which is funded by EPSRC (EP/L000202).

Supporting Information Available

Analysis of the localization of a core hole in a $2 \times 2 \times 1$ supercell of magnesium, full data for the experimental core electron binding energies and dielectric constants, plots showing the extrapolation of calculated core electron binding energies to the infinite supercell limit, k-point grids, finite size corrections, and full numerical results, relaxed structures, basis sets, and sample input files.

References

(1) Hait, D.; Head-Gordon, M. Highly Accurate Prediction of Core Spectra of Molecules at Density Functional Theory Cost: Attaining Sub-electronvolt Error from a Restricted Open-Shell Kohn–Sham Approach. *J. Phys. Chem. Lett.* **2020**, *11*, 775–786.

(2) Kahk, J. M.; Lischner, J. Accurate absolute core-electron binding energies of molecules, solids, and surfaces from first-principles calculations. *Phys. Rev. Materials* **2019**, *3*, 100801.

(3) Pueyo Bellafont, N.; Viñes, F.; Illas, F. Performance of the TPSS Functional on Predicting Core Level Binding Energies of Main Group Elements Containing Molecules: A Good Choice for Molecules Adsorbed on Metal Surfaces. *J. Chem. Theory Comput.* **2016**, *12*, 324–331.

(4) van Setten, M. J.; Costa, R.; Viñes, F.; Illas, F. Assessing GW Approaches for Predicting Core Level Binding Energies. *J. Chem. Theory Comput.* **2018**, *14*, 877–883.

(5) Golze, D.; Keller, L.; Rinke, P. Accurate Absolute and Relative Core-Level Binding Energies from GW. *J. Phys. Chem. Lett.* **2020**, *11*, 1840–1847.

(6) Golze, D.; Wilhelm, J.; van Setten, M. J.; Rinke, P. Core-Level Binding Energies from GW : An Efficient Full-Frequency Approach within a Localized Basis. *J. Chem. Theory Comput.* **2018**, *14*, 4856–4869.

(7) Ozaki, T.; Lee, C.-C. Absolute Binding Energies of Core Levels in Solids from First Principles. *Phys. Rev. Lett.* **2017**, *118*, 026401.

(8) Walter, M.; Moseler, M.; Pastewka, L. Offset-corrected Delta-Kohn-Sham scheme for semiempirical prediction of absolute x-ray photoelectron energies in molecules and solids. *Phys. Rev. B* **2016**, *94*, 041112.

(9) Aoki, T.; Ohno, K. Accurate quasiparticle calculation of x-ray photoelectron spectra of solids. *J. Phys.: Condens. Matter* **2018**, *30*, 21LT01.

(10) Zhu, T.; Chan, G. K.-L. All-Electron Gaussian-Based $G_0 W_0$ for Valence and Core Excitation Energies of Periodic Systems. *J. Chem. Theory Comput.* **2021**, *17*, 727–741.

(11) Kahk, J. M.; Lischner, J. Core electron binding energies of adsorbates on Cu(111) from first-principles calculations. *Phys. Chem. Chem. Phys.* **2018**, *20*, 30403–30411.

(12) Regoutz, A.; Wolinska, M. S.; Fernando, N. K.; Ratcliff, L. E. A combined density functional theory and x-ray photoelectron spectroscopy study of the aromatic amino acids. *Electron. Struct.* **2020**, *2*, 044005.

(13) Ljungberg, M.; Mortensen, J.; Pettersson, L. An implementation of core level spectroscopies in a real space Projector Augmented Wave density functional theory code. *J. Electron. Spectrosc.* **2011**, *184*, 427–439.

(14) Lembinen, M.; Nõmmiste, E.; Ers, H.; Docampo-Álvarez, B.; Kruusma, J.; Lust, E.; Ivaništšev, V. B. Calculation of core-level electron spectra of ionic liquids. *Int. J. Quantum Chem.* **2020**, *120*.

(15) Liu, J.; Matthews, D.; Coriani, S.; Cheng, L. Benchmark Calculations of K-Edge Ionization Energies for First-Row Elements Using Scalar-Relativistic Core–Valence-Separated Equation-of-Motion Coupled-Cluster Methods. *J. Chem. Theory Comput.* **2019**, *15*, 1642–1651.

(16) García-Gil, S.; García, A.; Ordejón, P. Calculation of core level shifts within DFT using pseudopotentials and localized basis sets. *Eur. Phys. J. B* **2012**, *85*, 239.

(17) Susi, T.; Mowbray, D. J.; Ljungberg, M. P.; Ayala, P. Calculation of the graphene C 1 s core level binding energy. *Phys. Rev. B* **2015**, *91*, 081401.

(18) Besley, N. A. Modeling of the spectroscopy of core electrons with density functional theory. *WIREs Comput. Mol. Sci.* **2021**, e1527.

(19) Viñes, F.; Sousa, C.; Illas, F. On the prediction of core level binding energies in molecules, surfaces and solids. *Phys. Chem. Chem. Phys.* **2018**, *20*, 8403–8410.

(20) Zheng, X.; Cheng, L. Performance of Delta-Coupled-Cluster Methods for Calculations of Core-Ionization Energies of First-Row Elements. *J. Chem. Theory Comput.* **2019**, *15*, 4945–4955.

(21) Klein, B. P.; Hall, S. J.; Maurer, R. J. The nuts and bolts of core-hole constrained ab initio simulation for K-shell x-ray photoemission and absorption spectra. *J. Phys.: Condens. Matter* **2021**, *33*, 154005.

(22) Bagus, P. S. Self-Consistent-Field Wave Functions for Hole States of Some Ne-Like and Ar-Like Ions. *Phys. Rev.* **1965**, *139*, A619–A634.

(23) Bagus, P. S.; Nelin, C. J.; Levchenko, S. V.; Zhao, X.; Davis, E. M.; Kuhlenbeck, H.; Freund, H.-J. Surface core level BE shifts for CaO(100): insights into physical origins. *Phys. Chem. Chem. Phys.* **2019**, *21*, 25431–25438.

(24) Bagus, P. S.; Nelin, C. J.; Zhao, X.; Levchenko, S. V.; Davis, E.; Weng, X.; Späth, F.; Papp, C.; Kuhlenbeck, H.; Freund, H.-J. Revisiting surface core-level shifts for ionic compounds. *Phys. Rev. B* **2019**, *100*, 115419.

(25) Blum, V.; Gehrke, R.; Hanke, F.; Havu, P.; Havu, V.; Ren, X.; Reuter, K.; Scheffler, M. Ab initio molecular simulations with numeric atom-centered orbitals. *Comput. Phys. Commun.* **2009**, *180*, 2175–2196.

(26) Knuth, F.; Carbogno, C.; Atalla, V.; Blum, V.; Scheffler, M. All-electron formalism for total energy strain derivatives and stress tensor components for numeric atom-centered orbitals. *Comput. Phys. Commun.* **2015**, *190*, 33–50.

(27) Havu, V.; Blum, V.; Havu, P.; Scheffler, M. Efficient integration for all-electron electronic structure calculation using numeric basis functions. *J. Comput. Phys.* **2009**, *228*, 8367–8379.

(28) Sun, J.; Ruzsinszky, A.; Perdew, J. Strongly Constrained and Appropriately Normed Semilocal Density Functional. *Phys. Rev. Lett.* **2015**, *115*, 036402.

(29) Strange, R.; Manby, F.; Knowles, P. Automatic code generation in density functional theory. *Comput. Phys. Commun.* **2001**, *136*, 310–318.

(30) Chang, C.; Pelissier, M.; Durand, P. Regular Two-Component Pauli-Like Effective Hamiltonians in Dirac Theory. *Phys. Scr.* **1986**, *34*, 394–404.

(31) van Lenthe, E.; Baerends, E. J.; Snijders, J. G. Relativistic total energy using regular approximations. *J. Chem. Phys.* **1994**, *101*, 9783–9792.

(32) Faas, S.; Snijders, J.; van Lenthe, J.; van Lenthe, E.; Baerends, E. The ZORA formalism applied to the Dirac-Fock equation. *Chem. Phys. Lett.* **1995**, *246*, 632–640.

(33) Yu, V. W.-z.; Corsetti, F.; García, A.; Huhn, W. P.; Jacquelin, M.; Jia, W.; Lange, B.; Lin, L.; Lu, J.; Mi, W. et al. ELSI: A unified software interface for Kohn–Sham electronic structure solvers. *Comput. Phys. Commun.* **2018**, *222*, 267–285.

(34) Yu, V. W.-z.; Campos, C.; Dawson, W.; García, A.; Havu, V.; Hourahine, B.; Huhn, W. P.; Jacquelin, M.; Jia, W.; Keçeli, M. et al. ELSI — An open infrastructure for electronic structure solvers. *Comput. Phys. Commun.* **2020**, *256*, 107459.

(35) Pulay, P. Convergence acceleration of iterative sequences. the case of scf iteration. *Chem. Phys. Lett.* **1980**, *73*, 393–398.

(36) Pulay, P. Improved SCF convergence acceleration. *J. Comput. Chem.* **1982**, *3*, 556–560.

(37) Kerker, G. P. Efficient iteration scheme for self-consistent pseudopotential calculations. *Phys. Rev. B* **1981**, *23*, 3082–3084.

(38) Bagus, P. S.; Schaefer, H. F. Localized and Delocalized 1s Hole States of the $O_2{}^+$ Molecular Ion. *J. Chem. Phys.* **1972**, *56*, 224–226.

(39) Ågren, H.; Jensen, H. J. A. An efficient method for the calculation of generalized overlap amplitudes for core photoelectron shake-up spectra. *Chem. Phys. Lett.* **1987**, *137*, 431–436.

(40) Michelitsch, G. S.; Reuter, K. Efficient simulation of near-edge x-ray absorption fine structure (NEXAFS) in density-functional theory: Comparison of core-level constraining approaches. *J. Chem. Phys.* **2019**, *150*, 074104.

(41) Chong, D. P. Localized and delocalized 1s core-holes in DFT calculations. *J. Electron Spectros. Relat. Phenomena* **2007**, *159*, 94–96.

(42) Gilbert, A. T. B.; Besley, N. A.; Gill, P. M. W. Self-Consistent Field Calculations of Excited States Using the Maximum Overlap Method (MOM). *J. Phys. Chem. A* **2008**, *112*, 13164–13171.

(43) Bagus, P. S.; Nelin, C. J.; Brundle, C. R.; Crist, B. V.; Lahiri, N.; Rosso, K. M. Combined multiplet theory and experiment for the Fe 2p and 3p XPS of FeO and Fe_2O_3. *J. Chem. Phys.* **2021**, *154*, 094709.

(44) Makov, G.; Payne, M. C. Periodic boundary conditions in *ab initio* calculations. *Phys. Rev. B* **1995**, *51*, 4014–4022.

(45) Castleton, C. W. M.; Höglund, A.; Mirbt, S. Managing the supercell approximation for charged defects in semiconductors: Finite-size scaling, charge correction factors, the band-gap problem, and the *ab initio* dielectric constant. *Phys. Rev. B* **2006**, *73*, 035215.

(46) Hine, N. D. M.; Frensch, K.; Foulkes, W. M. C.; Finnis, M. W. Supercell size scaling of density functional theory formation energies of charged defects. *Phys. Rev. B* **2009**, *79*, 024112.

(47) Lany, S.; Zunger, A. Accurate prediction of defect properties in density functional supercell calculations. *Modelling Simul. Mater. Sci. Eng.* **2009**, *17*, 084002.

(48) Lany, S.; Zunger, A. Assessment of correction methods for the band-gap problem and for finite-size effects in supercell defect calculations: Case studies for ZnO and GaAs. *Phys. Rev. B* **2008**, *78*, 235104.

(49) Freysoldt, C.; Neugebauer, J.; Van de Walle, C. G. Electrostatic interactions between charged defects in supercells: Electrostatic interactions between charged defects in supercells. *Phys. Status Solidi B* **2011**, *248*, 1067–1076.

(50) Freysoldt, C.; Grabowski, B.; Hickel, T.; Neugebauer, J.; Kresse, G.; Janotti, A.; Van de Walle, C. G. First-principles calculations for point defects in solids. *Rev. Mod. Phys.* **2014**, *86*, 253–305.

(51) Freysoldt, C.; Neugebauer, J. First-principles calculations for charged defects at surfaces, interfaces, and two-dimensional materials in the presence of electric fields. *Phys. Rev. B* **2018**, *97*, 205425.

(52) Wang, K.-L.; Gao, S.-P. Phonon dispersions, band structures, and dielectric functions of BeO and BeS polymorphs. *J. Phys. Chem. Solids* **2018**, *118*, 242–247.

(53) Shek, M.; Hrbek, J.; Sham, T.; Xu, G.-Q. A soft X-ray study of the interaction of oxygen with Li. *Surf. Sci.* **1990**, *234*, 324–334.

(54) Contour, J.; Salesse, A.; Froment, M.; Garreau, M.; Thevenin, J.; Warin, D. Analysis by Electron-Microscopy and XPS of Lithium Surfaces Polarized in Anhydrous Organic Electrolytes. *J. Microsc. Spect. Elec.* **1979**, *4*, 483–491.

(55) Wertheim, G.; Van Attekum, P.; Basu, S. Electronic structure of lithium graphite. *Solid State Commun.* **1980**, *33*, 1127–1130.

(56) Kowalczyk, S. P.; Ley, L.; McFeely, F. R.; Pollak, R. A.; Shirley, D. A. X-Ray Photoemission from Sodium and Lithium. *Phys. Rev. B* **1973**, *8*, 3583–3585.

(57) Powell, C. Elemental binding energies for X-ray photoelectron spectroscopy. *Appl. Surf. Sci.* **1995**, *89*, 141–149.

(58) Barrie, A.; Street, F. An Auger and X-ray photoelectron spectroscopic study of sodium metal and sodium oxide. *J. Electron. Spectrosc.* **1975**, *7*, 1–31.

(59) Citrin, P. H. High-Resolution X-Ray Photoemission from Sodium Metal and Its Hydroxide. *Phys. Rev. B* **1973**, *8*, 5545–5556.

(60) Jennison, D. R.; Weightman, P.; Hannah, P.; Davies, M. Calculation of Mg atom-metals XPS and Auger shifts using a Delta-SCF excited atom model. *J. Phys. C: Solid State Phys.* **1984**, *17*, 3701–3710.

(61) Yoshimura, K.; Yamada, Y.; Bao, S.; Tajima, K.; Okada, M. Degradation of Switchable Mirror Based on Mg–Ni Alloy Thin Film. *Jpn. J. Appl. Phys.* **2007**, *46*, 4260–4264.

(62) Ley, L.; McFeely, F. R.; Kowalczyk, S. P.; Jenkin, J. G.; Shirley, D. A. Many-body effects in x-ray photoemission from magnesium. *Phys. Rev. B* **1975**, *11*, 600–612.

(63) Peng, X.; Edwards, D.; Barteau, M. Reactions of O2 and H2O with magnesium nitride films. *Surf. Sci.* **1988**, *195*, 103–114.

(64) Darrah Thomas, T.; Weightman, P. Valence electronic structure of AuZn and AuMg alloys derived from a new way of analyzing Auger-parameter shifts. *Phys. Rev. B* **1986**, *33*, 5406–5413.

(65) Kieser, J.; Kleber, R. A new approach for the determination of the C ls binding energy. *Appl. Phys.* **1976**, *9*, 315–319.

(66) Johansson, G.; Hedman, J.; Berndtsson, A.; Klasson, M.; Nilsson, R. Calibration of electron spectra. *J. Electron. Spectrosc.* **1973**, *2*, 295–317.

(67) Xie, Y.; Sherwood, P. M. A. Ultrahigh Purity Graphite Electrode by Core Level and Valence Band XPS. *Surf. Sci. Spectra* **1992**, *1*, 367–372.

(68) Hamrin, K.; Johansson, G.; Gelius, U.; Nordling, C.; Siegbahn, K. Valence Bands and Core Levels of the Isoelectronic Series LiF, BeO, BN, and Graphite Studied by ESCA. *Phys. Scr.* **1970**, *1*, 277–280.

(69) Estrade-Szwarckopf, H.; Rousseau, B. Photoelectron core level spectroscopy study of Cs-graphite intercalation compounds—I. Clean surfaces study. *J. Phys. Chem. Solids* **1992**, *53*, 419–436.

(70) Koh, D.; Banerjee, S. K.; Locke, C.; Saddow, S. E.; Brockman, J.; Kuhn, M.; King, S. W. Valence and conduction band offsets at beryllium oxide interfaces with silicon carbide and III-V nitrides. *J. Vac. Sci. Technol. B* **2019**, *37*, 041206.

(71) Henck, H.; Pierucci, D.; Fugallo, G.; Avila, J.; Cassabois, G.; Dappe, Y. J.; Silly, M. G.; Chen, C.; Gil, B.; Gatti, M. et al. Direct observation of the band structure in bulk hexagonal boron nitride. *Phys. Rev. B* **2017**, *95*, 085410.

(72) Gaowei, M.; Muller, E. M.; Rumaiz, A. K.; Weiland, C.; Cockayne, E.; Jordan-Sweet, J.; Smedley, J.; Woicik, J. C. Annealing dependence of diamond-metal Schottky barrier heights probed by hard x-ray photoelectron spectroscopy. *Appl. Phys. Lett.* **2012**, *100*, 201606.

(73) McFeely, F. R.; Kowalczyk, S. P.; Ley, L.; Cavell, R. G.; Pollak, R. A.; Shirley, D. A. X-ray photoemission studies of diamond, graphite, and glassy carbon valence bands. *Phys. Rev. B* **1974**, *9*, 5268–5278.

(74) Kono, S.; Kodama, H.; Ichikawa, K.; Yoshikawa, T.; Abukawa, T.; Sawabe, A. Electron spectro-microscopic determination of barrier height and spatial distribution of Au and Ag Schottky junctions on boron-doped diamond (001). *Jpn. J. Appl. Phys.* **2014**, *53*, 05FP03.

(75) Maier, F.; Ristein, J.; Ley, L. Electron affinity of plasma-hydrogenated and chemically oxidized diamond (100) surfaces. *Phys. Rev. B* **2001**, *64*, 165411.

(76) Bermudez, V. M. Growth and structure of aluminum films on (001) silicon carbide. *J. Appl. Phys.* **1988**, *63*, 4951–4959.

(77) Waldrop, J. R.; Grant, R. W. Formation and Schottky barrier height of metal contacts to beta-SiC. *Appl. Phys. Lett.* **1990**, *56*, 557–559.

(78) King, S. W.; Davis, R. F.; Ronning, C.; Nemanich, R. J. Valence band discontinuity of the (0001) 2H-GaN / (111) 3C-SiC interface. *J. Electron. Mater.* **1999**, *28*, L34–L37.

(79) Yu, E. T.; Croke, E. T.; McGill, T. C.; Miles, R. H. Measurement of the valence-band offset in strained Si/Ge (100) heterojunctions by x-ray photoelectron spectroscopy. *Appl. Phys. Lett.* **1990**, *56*, 569–571.

(80) Puthenkovilakam, R.; Chang, J. P. Valence band structure and band alignment at the ZrO2/Si interface. *Appl. Phys. Lett.* **2004**, *84*, 1353–1355.